ELSEVIER

Biophysical Chemistry 130 (2007) 132–138

Biophysical Chemistry

http://www.elsevier.com/locate/biophyschem

Adsorption kinetics of c-Fos and c-Jun to air–water interfaces

Maximiliano Del Boca [a], Thatyane Morimoto Nobre [b], Maria Elisabete Darbello Zaniquelli [b], Bruno Maggio [a], Graciela A. Borioli [a,*]

[a] *Centro de Investigaciones en Química Biológica de Córdoba (CIQUIBIC, UNC - CONICET), Departamento de Química Biológica, Facultad de Ciencias Químicas, Universidad Nacional de Córdoba. Haya de la Torre y Medina Allende, Ciudad Universitaria, X5000HUA, Córdoba. Argentina*

[b] *Departamento de Química, Faculdade de Filosofia Ciencias e Letras de Ribeirão Preto, Universidade de Sao Paulo, Ribeirão Preto, Brazil*

Received 29 June 2007; received in revised form 17 August 2007; accepted 20 August 2007
Available online 25 August 2007

Abstract

The kinetics of adsorption to air–water interfaces of the biomembrane active transcription factors c-Fos, c-Jun and their mixtures is investigated. The adsorption process shows three distinct stages: a lag time, a fast pseudo zero-order stage, and a halting stage. The initial stage determines the course of the process, which is concentration dependent until the end of the fast stage. We show that c-Fos has faster adsorption kinetics than c-Jun over all three stages and that the interaction between both proteins is apparent in the adsorption profiles of the mixtures. Protein molecular reorganization at the interface determines the transition to the final adsorption stage of the pure proteins as well as that of the mixtures.

Keywords: Pending drop; Monolayer; Transcription factor; Protein adsorption

1. Introduction

Transcription factors are proteins that regulate gene expression, and many require dimerization prior to entering the nucleus to achieve their task. The b-ZIP (basic region leucine zipper) family is a major class among them [1]. The wide variety of targets is a hallmark of the b-ZIP dimers that requires a very strict regulation of specificity. Indeed, the coiled–coil interaction between the partners, even in the absence of DNA, is sufficient for specificity although perhaps not for stability [2,3]. c-Fos and c-Jun are well known b-ZIP transcription factors that form AP-1 heterodimers involved both in normal and oncogenic processes within cells. They have been widely studied in the context of their binding to DNA, but they can also associate to phospholipids and meddle with membrane function [4,5]. Indeed, c-Fos normally associates to endoplasmic reticulum membrane to modulate phospholipid metabolism [6,7], and it has been shown that it modulates phospholipase activity through changes of the phospholipid organization [8–11]. Both c-Fos and c-Jun interact with model lipid membranes individually, and are optimally stabilized in equimolar ratio by an air–water interface [4,5]. Most recently, a direct interaction of c-Fos with a non transcription factor protein, lamin A/C, is postulated as a mechanism for c-Fos sequestration at the nuclear envelope [12], widening the possibilities for regulation of its subcellular localization through interaction with membranes and therefore, of its function.

The kinetics of dimerization has been implicated in the biological functions of transcription complexes [2,13] and constitutes a different level of regulation, not only of b-ZIP function as such, but also of any function not related to transcription that might be attributed to the monomers. A delicate balance between dimerization and binding of c-Fos and c-Jun is exemplified by kinetics studies of adsorption of these proteins to DNA, which showed that the monomers first bind rapidly to DNA sequentially and then dimerize, while dimerization followed by binding to DNA occurs more slowly [14]. The kinetics of adsorption of c-Fos and c-Jun to interfaces is therefore a key component of the energetic landscape that drives their function.

We have investigated the kinetics of adsorption of c-Fos and c-Jun to an air–water interface, as a straightforward model to study protein interactions and dynamics, including formation of c-Fos/c-Jun heterodimers. Unlike most previous studies, performed either using peptides representing only the bZIP portion of both proteins [14,15] or the whole proteins in cells thereby

* Corresponding author. Tel.: +54 351 4334171x220; fax: +54 351 4334074 or 4334168.
E-mail address: gborioli@dqb.fcq.unc.edu.ar (G.A. Borioli).

0301-4622/$ - see front matter © 2007 Elsevier B.V. All rights reserved.
doi:10.1016/j.bpc.2007.08.005

imposing many interactions with cellular components [16–18], we have used full-length proteins in model membranes that allow reasonable control of the system. We extended our studies to cover the kinetics of interfacial adsorption of c-Fos, c-Jun and mixtures of both proteins using harmonic drop oscillation and axisymmetric analysis [19,20]. With this technique we were able to discriminate three kinetic stages: a lag time, a fast pseudo zero-order stage, and a halting stage, that are similar to those previously described for protein adsorption to oil water interface [21]. The initial approaching of molecules to the interface determines the course of the process, which is dependent on subphase concentration until the end of the fast stage. Our results indicate that c-Fos has faster adsorption kinetics than c-Jun over all three stages. The interaction between both proteins facilitates the adsorption whereas their molecular reorganization conditions the transition of the mixtures to the final stage of the process.

2. Experimental

Solutions were freshly prepared using dust free Milli-Q® water (surface tension of 72.8 mN/m and resistivity of 18.2 MΩ.cm). All other reagents were of the highest commercially available purity. His-tagged c-Jun and c-Fos were purified by affinity chromatography as previously described[4]. Protein stock solutions were in a buffer containing NaCl 0.5 M, Tris–HCl 20 mM, imidazole 300 mM, and urea 8 M, pH 7.4. The apparent molecular mass was taken as 42 kDa for c-Jun (334 aa) and 56 kDa for c-Fos (380 aa) according to Del Boca and col. [5]. The experiments were performed always in a NaCl 145 mM solution and at 20 °C. Absence of surface-active impurities in the subphase and in the spreading solvents was routinely controlled [5].

Radiolabelling of proteins was carried out by stoichiometric iodination with Chloramine-T as described elsewhere [22]. Iodine-125 Radionuclide, 1 mCi, (pH 8–11) (Reductant Free) was purchased from NEN Life Science. The radiolabelled proteins have the same behavior in π vs area compression isotherms as the unlabelled ones (not shown).

Interfacial tension was determined using two different methodologies: We use a pendant drop apparatus to study the kinetic of surface tension changes induced by protein adsorption. Gibbs and Langmuir monolayers were used to correlate other surface parameters with the interfacial tension vs. time curves, assuming that for a determined adsorption entity, independently of the methodology used to measure, at the same surface tension the system has the same molecular organization.

Pendant drop: Surface tension (γ) was determined using the pendant drop method with axisymmetric drop shape analysis (ADSA) [19] employing an optical contact angle meter, OCA-20, from Dataphysics Instruments GmbH, Germany. A drop of liquid, formed from a syringe into a thermostated optical glass cuvette containing water in the bottom to avoid drop evaporation, is imaged using a CCD camera. Specific software that uses a suitable position for a reference line in the image field was accessed to trigger the recording of the images even before the complete drop formation. The zero time was defined after playing the movie by selecting the suitable images and surface tension was determined by first digitizing and analyzing the profile of the droplet. Then, the Young–Laplace equation was fitted to the shape of the drops:

$$\Delta P = (\rho_d - \rho_l)\mathrm{gh} = (\gamma/R_1) + (\gamma/R_2)$$

where ΔP is the difference of pressure across the interface, ρd−ρl are the densities of the denser and the lighter stages respectively, g is the gravity acceleration constant, h is the height of the liquid column at the drop and $R_{1+}R_2$ the two main drop curvature radii [19].

Gibbs and Langmuir monolayers: Surface pressure (π) was measured by a platinized-Pt sensing plate connected to a surface pressure transducer. Surface potential (ΔV) was measured by a high impedance millivoltmeter connected to a surface ionizing ^{241}Am electrode positioned 5 mm above the monolayer surface, and to a reference calomel electrode submerged in the aqueous subphase. The kinetics of adsorption of radiolabelled proteins at the air-buffer interface was studied using a surface radiotracer method. Briefly, the rate of change of protein concentration at the air-buffer interface of radiolabelled protein solutions in a Teflon trough was monitored by measuring the surface radioactivity using a circular gas-probe detector with an active area of 6.4 cm^2 and a Geiger (Ludlum Measurements, Inc., Sweetwater, TX). The gas-probe detector was placed at about 4 mm from the surface of the liquid in the trough. The contribution of bulk radioactivity was abolished injecting the problem solution on a 18 ml teflon compartment with a surface area of 18 cm^2 connecting by a slit of 3 mm depth and an area of 25 mm^2 with a compartment of 36 ml and 36 cm^2 of surface area (Mayer Feintechnik, Germany) where the surface Geiger was placed. Control experiments were performed covering the surface of the slit and no signal was registered in the experimental time.

In Gibbs monolayers, π and ΔV vs. time isotherms were obtained injecting less than 70 μl of protein solution in the subphase of a 18 ml teflon compartment with a surface area of 18 cm^2 (Mayer Feintechnik, Germany), π and surface radioactivity vs. time isotherms were obtained injecting less than 70 μl of radiolabelled protein solution in the subphase of the sister compartment described above.

Langmuir monolayers were used to obtain the equilibrium surface compressibilities (Cs) of c-Fos, c-Jun and mixtures monolayers, π–area compression isotherms were carried out in a trough of 80 ml and a total area of 80 cm^2; aliquots of less than 60 μl of a cloroform:methanol:protein buffer solution (1:1:1/6) with a final protein concentration around 0.16 μg/ml were spread onto the surface, and after 10 min of equilibration the π–area curves were obtained as previously described [5]. Monolayer compressibilities were obtained from the surface pressure–mean molecular area isotherms as:

$$C_S = -(1/A)(dA/d\pi)$$

where Cs is the compressibility and A the molecular area at each surface pressure point of the isotherm. The interfacial elastic modulus of area compressibility, reflecting variations of the film in-plane elasticity, was calculated as $K = 1/Cs$. It was shown by Li and col. [23] that experimentally obtained K values are highly reproducible and, together with variations of the

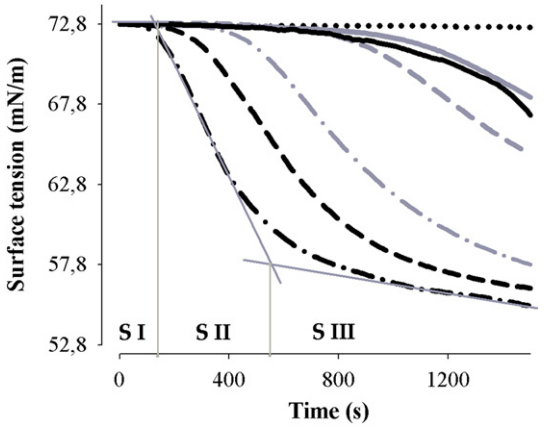

Fig. 1. Lateral surface tension changes relative to clean buffer (dotted line) with time, during adsorption of c-Fos (black) or c-Jun (gray) at 100 (full lines), 150 (stripped lines) and 200 (dot-strips) nM concentration in subphase. The adsorption profiles of both proteins at concentrations above 300 nM do not exhibit further changes. The three stages of the adsorption process, SI, SII and SIII are indicated. For concentrations below 150 nM the later stages develop over longer times than those shown here.

surface potential, can be reliably used to detect monolayer phase transitions and pre-collapse behavior.

3. Results and discussion

3.1. c-Fos and c-Jun adsorption kinetic stages. Pendant drop studies

The pendant drop system allowed us to resolve the adsorption kinetics of c-Fos and c-Jun into three kinetic stages as evidenced by defined slope changes in the surface pressure vs. time plot (Fig. 1). These stages correspond to an initial period of adsorption (SI), a relatively fast and linear pseudo steady-state adsorption (SII) and a gradual halting of the process (SIII). SI, SII and SIII reflect distinct molecular processes involved in the formation of a film at the interface, and are present for both proteins independently of the subphase concentration. The slope of the SII stage depends inversely on the SI time length (the shorter SI, the faster SII), suggesting that events taking place during the initial SI stage condition the evolution of the process. The correlation between the induction time (stage SI) and the adsorption itself (stage SII), is not a general observation, as can be seen for other systems described in the literature [24,25]. In our case, the larger the induction time, the higher is $d\gamma/dt$ at the step II as observed in Fig. 1, for which the more surface active c-Fos shows shorter induction times and highest $d\gamma/dt$, or adsorption rate.

The SI stage is a lag time corresponding to a progressive increment in concentration in the vicinity of the interface accompanied by small or practically no changes in π, as the protein is accumulating in the subsurface layer in the concept of Ward and Tordai [26]. The lack of π increment during SI means that the molecules should undertake a suitable conformation prior to or while being adsorbed. Hence, the length of SI depends not only on subphase concentration as predicted by the Fick's laws for a diffusion controlled process [27], but also on the nature of the molecules. It is also possible to observe from Fig. 1 that the subphase concentration range used in this work encompasses the critical concentration c* [28,29]. At c* the surface pressure change is maximal and for soluble proteins remains almost constant despite an increase in the bulk concentration; c* is 150 nM for c-Fos and 200 nM for c-Jun (data not shown), indicating that the former is more surface active than the latter. Indeed, c-Fos shows faster adsorption than c-Jun in the range of 100–200 nM: for c-Fos, SI-SII and SII-SIII transitions occur earlier, and the SII phase has higher slope than for c-Jun. These differences can be attributed to the conformational changes coupled with adsorption to the interface, that may contribute different amounts of energy for c-Fos and c-Jun. In this regard, it should be noted that measured molecular areas at the interface showed that c-Fos, although having higher MW, occupies smaller areas at the interface at all surface pressures and has a higher affinity for the interface compared to c-Jun [5]; this is an indication of the different extent of conformational changes due to adsorption in each case. Dimerization may also influence the adsorption kinetics differences between both proteins, since c-Jun forms homodimers in solution whereas c-Fos does not [2,3].

Once the number of molecules in the subsurface layer attains a threshold, the adsorption process enters the SII stage, during which a defined amount of surface area needs to be cleared to undergo interfacial insertion. In order to estimate this area we will consider desorption at this point negligible, which is valid at low surface pressures [30]. The adsorption rate to the interface can be described by the equation [31]

$$d\Gamma/dt = k_{ads}C_0\exp(-\pi\Delta A/kT), \quad (1)$$

where Γ is the surface concentration obtained from the compression isotherm of Langmuir monolayers at each surface pressure assuming that the molecular ordering is equivalent to that of Gibbs monolayers [31,32], k_{ads} is the rate constant for adsorption, C_0 is the concentration in the subphase, π is the surface pressure, ΔA is the cleared adsorption area allowing interfacial insertion, k is the Boltzmann constant and T is the

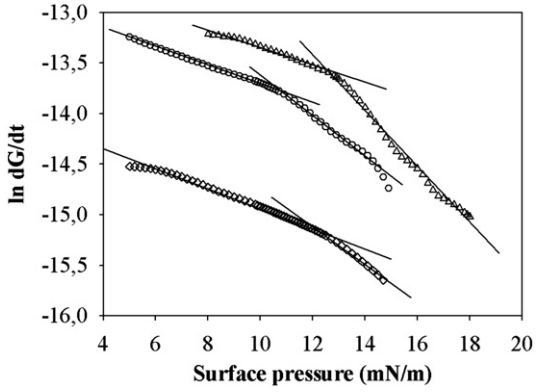

Fig. 2. Adsorption rates as a function of surface lateral pressure π for c-Fos (circles), c-Jun (diamonds) and an equimolar mixture of both proteins (triangles). Subphase concentration was 200 nM in all cases. Regression lines are shown ($R^2 > 0.98$). π is the initial surface tension minus the surface tension at each time point of the adsorption curves in Fig. 1. The surface excess quantities are calculated from Langmuir isotherms.

temperature. Here we use previously reported molecular area data from Langmuir monolayers for the obtention of surface concentration [4,5], which is strictly valid for insoluble proteins; however, c-Fos and c-Jun exhibit amphitropic properties and do not significantly desorb once deposited onto the interface [4,5]. The left hand term in the equation is the slope of the adsorption curve as a function of time at each surface pressure point, obtained from the tangent to the Gibbs isotherms in Fig. 1. The resulting adsorption rates $d\Gamma/dt$ as a function of π, of c-Fos and c-Jun for 200 nM concentration in the subphase are shown in Fig. 2. The slopes in each curve define two regions that correspond to stages SII and SIII, during which the molecules undergo conformational changes for area clearance and for final interface molecular disposition respectively. The rate constants for adsorption k_{ads} might in principle be obtained from these curves; however, the values of k_{ads} calculated with the available data are unreliable at very low surface pressures, and also render considerable errors in the quantification of SI. The molecular areas ΔA that need to be cleared for the protein interfacial insertion during the SII and SIII stages were calculated from the slopes in Fig. 2.

The values of ΔA are equal for both proteins and approximately equivalent to 2–3 aminoacid residues in SII and 5–6 aminoacid residues in SIII, considering an area of 15 Å^2 per residue (Table 1); they are noticeably smaller than those reported in the literature for other proteins of various tertiary structures, ranging from 50 to 200 Å^2 [33–35], perhaps due to the characteristic bZIP domain that is likely to interact with the interface and which constitutes the only structurally defined – a short α helix – region in these proteins. The molecular energy available from the spontaneous organization of the interface, equivalent to the work W done for area clearance and reorganization, is also very small for both proteins over the whole process (Table 1), as is expected for flexible proteins such as c-Fos and c-Jun [36,37].

Finally, it is clear that the change in slope in the curves of Fig. 2 (i.e. the passage from SII to SIII) is less marked for c-Jun, indicating that its molecular reorganization and/or interfacial insertion is less cooperative than that of c-Fos, in coincidence with the Langmuir isotherms.

3.2. c-Fos adsorption kinetics stages. Monolayer studies

The monolayer data provide further information to evaluate the adsorption process. Although the kinetics is different in the Wilhelmy method than in the pending drop system due mainly to curvature effects and to different area/volume ratio [38], the adsorption process is similar and the three stages, SI, SII and SIII, can be observed in the isotherm of c-Fos adsorbed to a planar air–water interface from a 200 nM subphase concentration (Fig. 3).

Table 1
Cleared areas and work of c-Fos, c-Jun and the c-Fos/c-Jun equimolar mixture

	ΔA_1 (SII) (Å^2)[a]	W_1 (kcal/mol)[b]	ΔA_2 (SIII) (Å^2)[a]	W_2 (kcal/mol)[b]
c-Fos	37	0.564	87	0.550
c-Jun	39	0.701	83	0.299
Mixture 1:1	37	0.481	117	0.842

[a] ΔA_1 and ΔA_2 correspond to the interfacial areas cleared at SII and SIII adsorption stages respectively and were taken form the slopes in Fig. 2.

[b] $W1$ and $W2$ are the work done against the surface pressure interval at SII and SIII adsorption stages respectively, and were calculated as $\Delta\pi \times \Delta A$. Correlation coefficients are $R^2 > 0.98$.

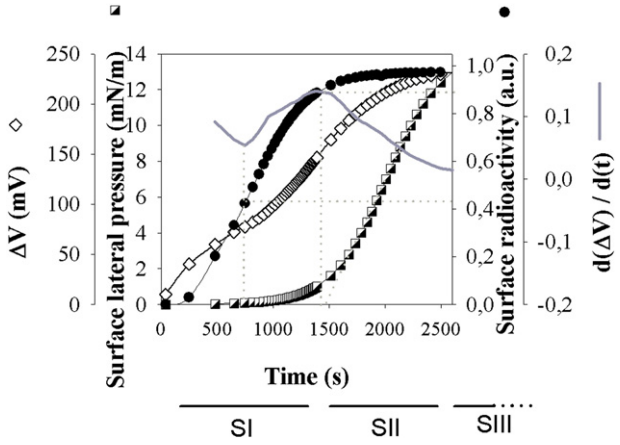

Fig. 3. Adsorption parameters dependence on adsorption time. Surface pressure (squares, inner left scale), surface potential (diamonds, outer left scale), surface radioactivity (circles, inner right scale) and deltaV/delta t changes (gray line, outer right scale) are plotted for c-Fos. The surface potential derivative with time emphasizes the changes in slope of the outer left scale curve. The dotted lines denote transition regions of interest. The lines below the graph show the SI, SII and SIII phases.

The same process was followed in a parallel experiment by the radiotracer technique, letting ^{125}I labelled c-Fos adsorb from a subphase of equal concentration. The radioactive probe allows to detect the molecules approaching the subsurface layer during the SI stage (within 10 min after the injection), which is also marked by a change in the surface potential profile. Not surprisingly, the changes of the surface radioactivity and of surface potential sense the adsorption already during the SI stage more readily than the surface pressure, probably due to the sampled regions by these techniques: surface pressure samples just the surface itself, whereas surface potential and radiotracing are also sensitive to the subsurface region. At about 40% of total adsorbed molecules, as measured by radioactivity detection, there is a change in the thermodynamic environment at the interface that could be ascribed to coherent film formation. The transition from SI to SII occurs when about 90% of the molecules to be adsorbed are within the interfacial environment, in coincidence with the beginning of the raise in π. This transition can be clearly detected by radioactivity and by a slope change in the derivative of surface potential with time defined by $\left(\frac{\partial \Delta V}{\partial t}\right)_T$ (maximum of the curve) (Fig. 3). SII stage elapses as the molecules clear the surface area against the surface pressure barrier through conformational changes, as discussed earlier. The next transition, from SII to SIII, is coincident with a change of molecular organization at the interface previously described for c-Fos [4]. The SIII slow kinetics stage is associated to further conformational changes of the adsorbed molecules [39], and progresses without further increment in the number of molecules at the interface while they gradually acquire the final interfacial organization.

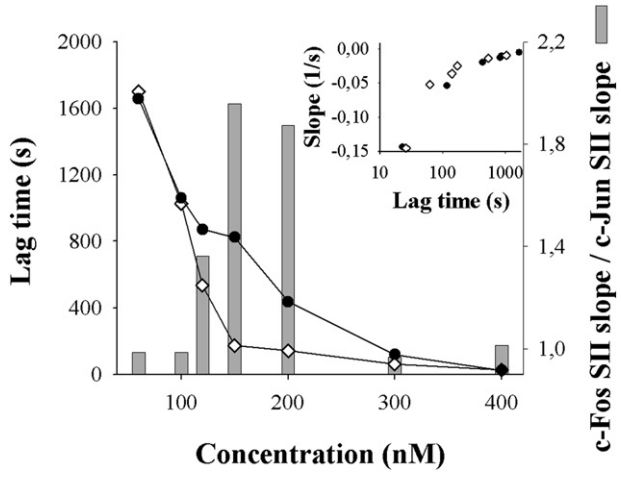

Fig. 4. Dependence of lag time on concentration (left scale) for c-Fos (white diamonds) and c-Jun (black circles), and of the ratio of c-Fos to c-Jun slopes in SII (gray bars, right scale). Inset: slope of SII as a function of the lag time. The symbols are the same as in the figure. The point values for the symbols and the bars are taken from curves like the ones shown in Fig. 1.

3.3. Dependence of the adsorption kinetics on concentration and on protein identity. Pendant drop studies

The lag time (SI stage) is determinant of the fast kinetic stage (inset in Fig. 4) and its length depends on subphase concentration at intermediate concentrations below 100 nM and above 300 nM, but depends on the identity of the protein being adsorbed within this concentration range (Fig. 4) SII kinetics concordantly (Fig. 4, right scale) shows greater differences for the two proteins in the same range of intermediate subphase concentrations. These observations mean that the process can be explained by simple diffusion (based mainly on kinetic factors) at low or high surface coverage whereas for intermediate concentrations, the adsorption energy barrier is more readily overcome by c-Fos.

The SII/SIII transition depends on subphase concentration, with the same pattern as for the lag time: c-Fos enters the slow SIII stage earlier than c-Jun at intermediate concentrations (Fig. 5, left scale, empty symbols). Conversely, the surface pressure point for this transition is independent of concentration (Fig. 5, right scale,

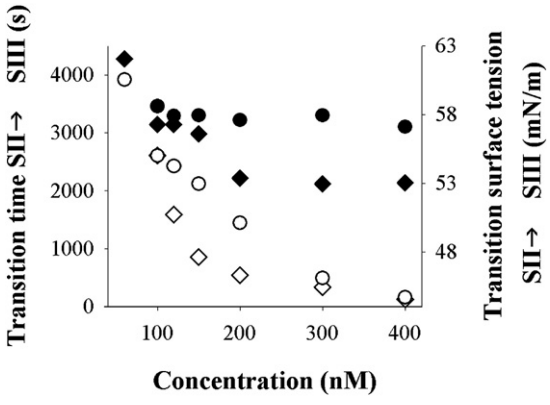

Fig. 5. Dependence of the SII–SIII transition (left scale, empty symbols) and of the corresponding surface lateral tension (right scale, full symbols) on concentration, for c-Fos (diamonds) and c-Jun (circles).

Table 2
Surface tension values for the SII → SIII transition and for interfacial reorganization due to compression

		Surface tension for the SII → SIII transition[a] (mN/m)		Interfacial reorganization[b] (mN/m)	
		γ	π	γ	π
c-Fos		57.5±0.4	15.3±0.4	56.3±1	16.5±1
c-Jun		53.4±0.5	19.4±0.5	52.9±1	19.9±1
Mixture	0.71	55.2±0.4	17.6±0.4	55.5±1	17.3±1
(c-Fos mole fraction)	0.5	55.5±0.4	17.3±0.4	57±1	15.8±1
	0.29	55.6±0.4	17.2±0.4	56.5±1	16.3±1

[a]Values were taken from Fig. 6. [b]Values of π were obtained from Langmuir isotherms as defined in the Experimental section. The corresponding surface tension γ values were calculated as $\gamma = \gamma_0 - \pi$.

full symbols) and, again, adopts a constant value coincident with that of the previously reported molecular reorganization of each protein [4,5] that takes place when pure c-Fos or c-Jun monolayers are compressed beyond 11–15 mN/m and 11–20 mN/m respectively (Table 2). This observation agrees with that derived from c-Fos monolayer experiments discussed earlier.

3.4. Adsorption kinetics of mixtures. Pendant drop studies

To elucidate if the interaction between c-Fos and c-Jun affects adsorption, we looked at the adsorption kinetics of mixtures with different proportions of each protein (Fig. 6). The analysis reveals that: 1) All mixtures have a faster adsorption kinetics than expected based on the individual behavior of the proteins; 2) c-Fos gravitates most in the adsorption behavior of the mixtures, because the one having an excess of c-Fos adsorbs most readily; 3) However, it does so even faster than this faster component alone, indicating that the interaction between c-Fos and c-Jun also influences their conjunct adsorption; 4) Similar

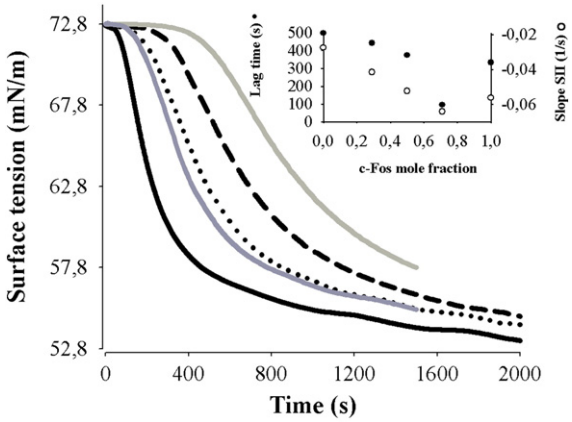

Fig. 6. Lateral surface tension variation during adsorption of c-Fos/c-Jun mixtures with the indicated proportions (straight line: 2.5 c-Fos:1 c-Jun; dotted line: 1 c-Fos:1 c-Jun; dashed line: 1c-Fos:2.5 c-Jun) as a function of time. The variation of the same parameter for the pure proteins (c-Fos: dark gray, c-Jun: light gray) is shown to facilitate comparison. Inset: dependence of initial and fast stage adsorption kinetics with composition for c-Fos/c-Jun mixtures. The lag time length (empty circles, left scale) and the SII slope (full circles, right scale) of adsorption curves of mixtures with different compositions are plotted. Protein concentration in the subphase is 200 nM for all curves.

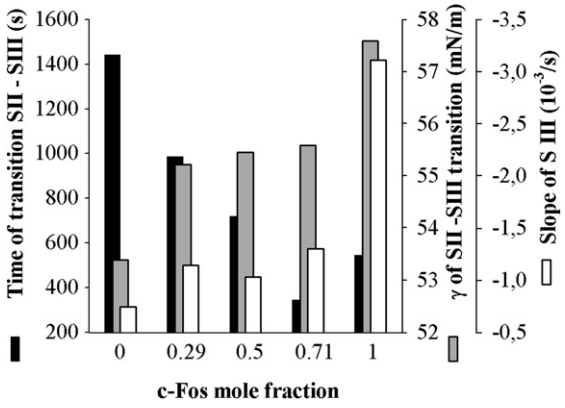

Fig. 7. Dependence of the SII–SIII transition and of the SIII course, on composition for c-Fos/c-Jun mixtures. The time of SII–SIII transition (black bars, left scale), the surface tension (γ) at which this transition occurs (gray bars, near right scale) and the slope of SIII stage (white bars, far right scale) are plotted as a function of the mole fraction of c-Fos in the mixture.

to the pure proteins, the initial SI or lag time of the mixtures dictates the kinetics of stage SII so that the shorter the lag time, the greater the slope of the adsorption curve in the range of the fast stage (Inset in Fig. 6).

It is clear then that the faster kinetics of c-Fos is a main factor determining the adsorption kinetics of the mixtures, and that the interaction with c-Jun further aids the process, carrying it to be even faster than pure c-Fos. This is true for the initial and fast stages up to the time point of SII-SIII transition, which in the c-Fos enriched mixture happens even earlier than for this fastest adsorbing component alone (Fig. 7, left scale). On the other hand, the surface tension at which this transition occurs is independent of composition, with a same value for all mixtures that is intermediate between those of the two pure components (Fig. 7 near right scale and Table 2). We compared this parameter with the pressure for interfacial molecular reorganization, assessed by Langmuir isotherms as described in the Experimental section and in previous work [5], which for the pure proteins is related to the SII-SIII transition surface tension. It resembles more that of c-Fos at all mole fractions (Table 2), indicating that this protein dominates the molecular reorganization in the mixtures. An interesting observation is that the behavior of the equimolar mixture, which was shown to be more stablilized than other proportions [5], does not deflect substantially from the average trend of variation neither in the lag time nor in the slope of SII. Hence, there seems to be a preference for the proteins to adsorb to the interface rather than interact between them in the subphase in the course of SII. This is in agreement with the observation by Kohler and Scherpatz [14] of monomer binding to DNA followed by dimerization in a system that can be considered analogous. The model proposed by Lin and col. [40] in which the cohesive interaction at the interface favours the final stages of the adsorption process, where the highly populated interface allows a better molecular interaction, also supports our observations. At the last stage of adsorption, the slope of SIII for the mixtures is closer to that of c-Jun, so the less cooperative molecule to adopt the definitive configuration at the interface determines a slower rate of the halting stage (Fig. 7 far right scale).

4. Conclusions

- c-Fos exhibits faster adsorption kinetics than c-Jun.
- The interaction between c-Fos and c-Jun at the interface facilitates the adsorption of mixtures compared to each protein alone.
- The surface pressure of protein reorganization marks the SII-SIII kinetic transition to the final stage of the process.

Acknowledgments

We thank CONICET, FONCyT and SECyT-UNC from Argentina, CNPQ from Brazil, and CAPES-SECyT, for financial support. MDB is a fellow, BM and GAB are Career Investigators of CONICET, Argentina.

References

[1] Y. Fujii, T. Shimizu, T. Toda, M. Yanagida, Y. Hakoshima, Structural basis for the diversity of DNA recognition by bZIP transcription factors, Nat. Struct. Biol. 7 (2000) 889–893.
[2] C. Vinson, M. Myakishev, A. Acharya, A. Mir, J. Moll, M. Bonovich, Classification of human B-ZIP proteins based on dimerization properties, Mol. Cell. Biol. 22 (2002) 6321–6335.
[3] J.R. Newman, A.E. Keating, Comprehensive identification of human bZIP interactions with coiled-coil arrays, Science 300 (2003) 2097–2101.
[4] G.A. Borioli, B.L. Caputto, B. Maggio, c-Fos is surface active and interacts differentially with phospholipid monolayers, Biochem. Biophys. Res. Commun. 280 (2001) 9–13.
[5] M. Del Boca, B.L. Caputto, B. Maggio, G.A. Borioli, c-Jun interacts with phospholipids and c-Fos at the interface, J. Colliod. Interface. Sci. 287 (2005) 80–84.
[6] D.F. Bussolino, M.E. Guido, G.A. Gil, G.A. Borioli, M.L. Renner, V.R. Grabois, C.B. Conde, B.L. Caputto, c-Fos associates with the endoplasmic reticulum and activates phospholipid metabolism, The FASEB J. 15 (2001) 556–558.
[7] G.A. Gil, D.F. Bussolino, M.M. Portal, A.A. Pecchio, M.L. Renner, G.A. Borioli, M.E. Guido, B.L. Caputto, c-Fos activated phospholipid synthesis is required for neurite elongation in differentiating PC12 cells, Mol. Biol. Cell. 15 (2004) 1881–1894.
[8] G.A. Borioli, M.L. Fanani, B.L. Caputto, B. Maggio, Fos is a surface pressure-dependent diverter of phospholipase activity, Biochem. Biophys. Res. Commun. 295 (2002) 964–969.
[9] G.A. Borioli, B.L. Caputto, B. Maggio, Phospholipase activity is modulated by c-Fos through substrate expansion and hyperpolarization, FEBS Lett. 570 (2004) 82–86.
[10] G.A. Borioli, B.L. Caputto, B. Maggio, c-Fos and phosphatidylinositol – 4,5-biphosphate reciprocally reorganize in mixed monolayers, Biochim. Biophys. Acta 1668 (2005) 41–52.
[11] G.A. Borioli, B. Maggio, The surface thermodynamics reveals selective structural information storage capacity of c-Fos-phospholipid interactions, Langmuir 22 (2006) 1775–1781.
[12] C. Ivorra, M. Kubicek, J.M. Gonzalez, S.M. Sanz-Gonzalez, A. Alvarez-Barrientos, J.E. O'Connor, B. Burke, V. Andres, A mechanism of AP-1 suppression through interaction of c-Fos with lamin A/C, Genes Dev. 20 (2006) 307–320.
[13] C. Vinson, A. Acharya, E. Taparowsky, Deciphering B-ZIP transcription factor interactions in vitro and in vivo, Biochim. Biophys. Acta 1759 (2006) 4–12.
[14] J.J. Kohler, A. Schepartz, Kinetic studies of Fos-Jun-DNA complex formation: DNA binding prior to dimerization, Biochemistry 40 (2001) 130–142.
[15] R. Oyama, H. Takashima, M. Yonezawa, N. Doi, E. Miyamoto-Sato, M. Kinjo, H. Yanagawa, Protein–protein interaction analysis by C-terminally

specific fluorescence labeling and fluorescence cross-correlation spectroscopy, Nucl. Acids Res. 34 (2006) 102–109.
[16] K. Ogita, H. Okuda, M. Kitano, Y. Fujinami, K. Ozaki, Y. Moneda, Localization of activator protein-1 complex with DNA binding activity in mitochondria of murine brain after in vivo treatment with kainite, J. Neurosci. 22 (2002) 2561–2570.
[17] K. Chida, S. Nagamori, T. Kuroki, Nuclear translocation of Fos is stimulated by interaction with Jun through the leucine zipper, Cell. Mol. Life Sci. 55 (1999) 297–302.
[18] N. Baudendistel, G. Miller, W. Waldeck, P. Angel, J. Langowski, Two-hybrid fluorescence cross-correlation spectroscopy detects protein–protein interactions in vivo, Chem. Phys. Chem. 6 (2005) 984–990.
[19] P. Cheng, D. Li, L. Boruvka, Y. Rotenberg, A.W. Neumann, Automation of axisymmetric drop shape analysis for measurements of interfacial tensions and contact angles, Colloids Surf. 43 (1990) 151–167.
[20] L. Caseli, D.C. Masui, R.P.M. Furriel, F.A. Leone, M.E.D. Zaniquelli, Adsorption kinetics and dilatational rheological studies for the soluble and anchored forms of alkaline phosphatase at the air/water interface, J. Braz. Chem. Soc. 16 (2005) 969–977.
[21] C.J. Beverung, C.J. Radke, H.W. Blanch, Protein adsorption at the oil water interface: characterization of adsorption kinetics by dynamic interfacial tension measurements, Biophys. Chemist. 81 (1999) 59–80.
[22] B.W. O'Malley, J.G. Hardman, Methods in Enzimology, Academic Press, New York, 1975.
[23] X.-M. Li, J.M. Småby, M.M. Momsen, H.L. Brockman, R.E. Brown, Sphingomyelin interfacial behavior: the impact of changing acyl chain composition, Biophys. J. 78 (2000) 1921–1931.
[24] R. Miller, V.B. Fainerman, A.V. Makievski, J. Krägel, R. Wüstneck, Adsorption characteristics of mixed monolayers of a globular protein and a non-ionic surfactant, Colloids Surf., A 161 (2000) 151–157.
[25] L. Liggieri, M. Ferrari, A. Massa, F. Ravera, Molecular reorientation in the adsorption of some C_iE_j at the water–air interface, Colloids Surf., A 156 (1999) 455–463.
[26] A.F.H. Ward, L. Tordai, Time-dependence of boundary tensions of solutions, J. Phys. Chem. 14 (1946) 453–461.
[27] K.S. Birdi, Lipid and biopolymers monolayers at liquid interfaces, Plenum Press, New York, 1989, p. 197.
[28] J. Benjamins, J.A. Feijter, M.T.A. Evans, D.E. Graham, M.C. Phillips, Dynamic and static properties of proteins adsorbed at the air/water interface, Disc. Faraday Soc. 59 (1975) 218–229.
[29] R. Miller, V.B. Fainerman, E.V. Akesenenko, M.E. Leser, M. Michel, Dynamic surface tension and adsorption kinetics of β-Casein at the solution/air interface, Langmuir 20 (2004) 771–777.
[30] V.B. Fainerman, R. Miller, J.K. Ferri, H. Watzke, M.E. Leser, M. Michel, Reversibility and irreversibility of adsorption of surfactants and proteins at liquid interfaces, Adv. Colloid Interface Sci. 123–126 (2006) 163–171.
[31] S. Damodaran, K.B. Song, Kinetics of adsorption of proteins at interfaces: role of protein conformation in diffusional adsorption, Biochim. Biophys. Acta 954 (1988) 253–264.
[32] M. Cejudo Fernández, C. Carrera Sánchez, M.R. Rodríguez Niño, J.M. Rodríguez Patiño, The effect of monoglycerides on structural and topographical characteristics of adsorbed β-Casein films at the air–water interface, Biomacromolecules 7 (2006) 507–514.
[33] D.E. Graham, M.C. Phillips, Proteins at liquid interfaces: I. Kinetics of adsorption and surface denaturation, J. Colloid Interface Sci. 70 (1979) 403–414.
[34] L. Ter-Minassian-Saraga, Protein denaturation on adsorption and water activity at interfaces: an analysis and suggestion, J. Colloid Interface Sci. 80 (1981) 393–401.
[35] F. MacRitchie, Chemistry at Interfaces, Academic Press, San Diego, 1990, p. 160.
[36] L. Iakoucheva, C.J. Brown, J.D. Lawson, Z. Obradovic, A.K. Dunker, Intrinsic disorder in cell-signaling and cancer-associated proteins, J. Mol. Biol. 323 (2002) 573–584.
[37] C.S. Rao, S. Damodaran, Is surface pressure a measure of interfacial water activity? Evidence from protein adsorption behavior at interfaces, Langmuir 16 (2000) 9468–9477.
[38] R. Miller, V.B. Fainerman, A.V. Makievski, M.E. Leser, M. Michel, E.V. Aksenenko, Determination of protein adsorption by comparative drop and bubble profile analysis tensiometry, Colloids Surf., B (2004) 36–123.
[39] A.P.J. Middelberg, C.J. Radke, H.W. Blanch, Peptide interfacial adsorption is kinetically limited by the thermodynamic stability of self association, Proc. Natl. Acad. Sci. 97 (2000) 5054–5059.
[40] S-H. Lin, K. McKeigue, C. Maldarelli, Effect of cohesive energies between adsorbed molecules on surfactant exchange processes: shifting from diffusion control for adsorption to kinetic-diffusive control for re-equilibration, Langmuir 10 (1994) 3442–3448.